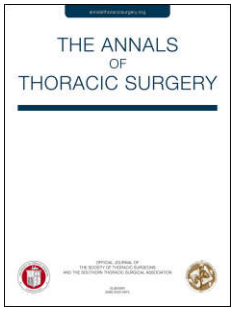

Shear Stress and Aortic Strain Associations with Biomarkers of Ascending Thoracic Aortic Aneurysm

Salvatore Pasta, PhD, Valentina Agnese, PhD, Alessia Gallo, PhD, Federica Cosentino, PhD, Marzio Di Giuseppe, PhD, Giovanni Gentile, MD, Giuseppe M. Raffa, MD, PhD, Joseph F. Maalouf, MD, Hector I. Michelena, MD, Diego Bellavia, PhD, MD, Pier Giulio Conaldi, MD, Michele Pilato, MD

PII: S0003-4975(20)30523-3

DOI: https://doi.org/10.1016/j.athoracsur.2020.03.017

Reference: ATS 33663

To appear in: *The Annals of Thoracic Surgery*

Received Date: 15 November 2019

Revised Date: 10 February 2020

Accepted Date: 5 March 2020

Please cite this article as: Pasta S, Agnese V, Gallo A, Cosentino F, Di Giuseppe M, Gentile G, Raffa GM, Maalouf JF, Michelena HI, Bellavia D, Conaldi PG, Pilato M, Shear Stress and Aortic Strain Associations with Biomarkers of Ascending Thoracic Aortic Aneurysm, *The Annals of Thoracic Surgery* (2020), doi: https://doi.org/10.1016/j.athoracsur.2020.03.017.

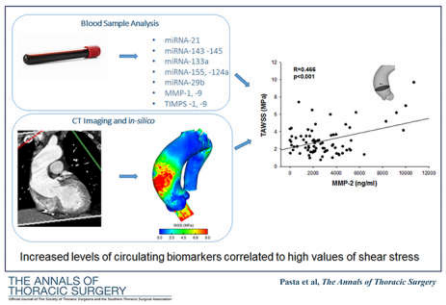

Increased levels of circulating biomarkers correlated to high values of shear stress

THE ANNALS OF THORACIC SURGERY

Pasta et al, *The Annals of Thoracic Surgery*

Shear Stress and Aortic Strain Associations with Biomarkers of Ascending Thoracic Aortic Aneurysm

Running head: Linking shear stress and biomarkers

Salvatore Pasta[1], PhD, Valentina Agnese[2], PhD, Alessia Gallo[3], PhD, Federica Cosentino[4], PhD, Marzio Di Giuseppe[4], PhD, Giovanni Gentile[5], MD, Giuseppe M Raffa[2], MD, PhD Joseph F. Maalouf[5], MD, Hector I. Michelena[5], MD, Diego Bellavia[2], PhD, MD, Pier Giulio Conaldi[3], MD, Michele Pilato[2], MD

[1] Bioengineering Division, Department of Engineering, University of Palermo, Palermo, Italy

[2] Department for the Treatment and Study of Cardiothoracic Diseases and Cardiothoracic Transplantation, IRCCS-ISMETT, Palermo, Italy

[3] Department of Laboratory Medicine and Advanced Biotechnologies, IRCCS-ISMETT, Palermo, Italy

[4] Department of Department of Health Promotion, Mother and Child Care, Internal Medicine and Medical Specialties, University of Palermo, Palermo, Italy

[5] Department of Diagnostic and Therapeutic Services, Radiology Unit, IRCCS-ISMETT, Palermo, Italy

[6] Department of Cardiovascular Medicine, Mayo Clinic and Foundation, Rochester (MN), USA

Total Word count: 4498

Corresponding author:
Salvatore Pasta, PhD
Professor of Industrial Bioengineering,
Department of Engineering
University of Palermo
Email: salvatore.pasta@unipa.it

Abstract

Background: This study aims to investigate the association of wall shear stress (WSS) and aortic strain with circulating biomarkers including matrix metalloproteinases (MMPs), tissue inhibitors (TIMPs) and exasomal level of miRNAs in ascending aortic aneurysms (AsAA) of patients with bicuspid or tricuspid aortic valve.

Methods: A total of 76 variables from 125 patients with ascending aortic aneurysms were collected from a) blood plasma to measure plasma levels of miRNAs and protein activity; b) computational flow analysis to estimate peak systolic WSS and time-average WSS (TAWSS); c) imaging analysis of computed-tomography angiography to determine aortic wall strain. Principal component analysis followed by logistic regression allowed to develop a predictive model of aortic surgery by combining biomechanical descriptors and biomarkers.

Results: The protein activity of MMP-1, TIMP-1 and MMP-2 was positively correlated to the systolic WSS and TAWSS observed in the proximal ascending aorta (eg, $R=0.52$, $p<0.001$, for MMP-1 with TAWSS) where local maxima of WSS were found. For bicuspid patients, aortic wall strain was associated with miR-26a ($R=0.55$, $p=0.041$) and miR-320a ($R=0.69$, $p<0.001$), which shown a significant difference between bicuspid and tricuspid patients. ROC curves revealed that the combination of WSS, MMP-1, TIMP-1 and MMP-12 is predictive of aortic surgery (AUC=0.898).

Conclusions: Increased flow-based and structural descriptors of AsAAs are associated to high levels of circulating biomarkers, implicating adverse vascular remodeling in the dilated aorta by mechanotransduction. A combination of shear stress and circulating biomarkers has the potential to improve the decision-making process of AsAAs towards a highly individualized level.

Keywords: ascending thoracic aortic aneurysm, bicuspid aortic valve, biomarkers

ABREVIATIONS

AA1=analysis plane at sino-tubular junction

AA2=analysis plane at mid-ascending aorta

AA3=analysis plane at distal ascending aorta

AsAA= ascending aortic aneurysms

AUC=area under the curve

BAV=bicuspid aortic valve

CTA=computed-tomography angiography

Dasc=diameter of ascending aorta

Ddias=diastolic aortic diameter

Dsinus=diameter of sinus of vasalva

DSTJ=diameter of sinotubular junction

Dsys=systolic aortic diameter

miRNA=micro ribonucleic acid

MMP=metalloproteinase

PCA=principal component analysis

Pdias=diastolic pressure

Psmod= pressure-strain modulus

Psys=systolic pressure

ROC=receiver operating characteristic

TAV=tricuspid aortic valve

TAWSS=time-average wall shear stress

TGF-β=transforming growth factor β

TIMP=tissue inhibitor

WSS=wall shear stress

An ascending aortic aneurysm (AsAA) is a potentially life threatening cardiovascular disease, associated to weakening of the aortic wall and risk of adverse complications. While AsAA has an incidence of 10/100,000 persons per year in the general population [1], approximately 40% of patients with bicuspid aortic valve (BAV) have associated aortopathy (dilatation) in referral centers [2] (namely, BAV AsAA) and higher rate of aortic dissection than patients with tricuspid aortic valve (TAV) and aortic dilatation [3]. AsAAs are repaired by elective surgery on the basis of aortic size and growth rate, but rupture and dissection may occur at aortic diameters not falling within surgical guidelines.

The majority of research studies on the development of new risk-stratification criteria for AsAAs are based on: a) the development of novel imaging techniques to describe and quantify biomechanical properties such as flow-related mechanical stimuli and aortic wall strain; and b) the identification of circulating biomarkers to improve diagnosis and surveillance of aortic wall disease. Non-invasive biomarkers including transforming growth factor β (TGF-β) [4], matrix metalloproteinases (MMPs) and associated tissue inhibitors (TIMPs) [5, 6], miRNAs molecules [7] and endothelial progenitor cells [8] have been investigated and implicated in the pathogenesis of AsAA, leading to degradation of extracellular matrix (ECM) and increased aortic wall stiffness. Imaging based on 4D Flow MRI [9], *in-silico* computational modeling [10] or a combination of them [11] have confirmed an altered hemodynamic environment in BAV AsAA with well-functioning or stenotic valve leaflets [12]. The underlying hypothesis is that flow disturbances induce local wall shear stress (WSS) forces on the aortic wall, portending to adverse vascular remodeling. The study of Guzzardi and collaborators [13] is the only report showing a tight link between altered WSSs and regional aortic tissue remodeling in BAV AsAA. Elevated aortic WSS estimated by 4D Flow MRI in candidates for elective aortic resection corresponded to regions of severe dysregulation of ECM in aortic tissue samples as compared to regions of normal WSS in the same patient's aorta. More recently, the same group reported a

relationship between elastic fiber thinning and increased WSSs, particularly in the setting of aortic valve stenosis [14].

Using computational modeling and blood samples obtained from a large cohort of patients with AsAAs and different valve phenotypes, we sought to investigate the mechanistic link between biomechanical properties and circulating biomarkers. To enhance risk stratification to high level, logistic regression based on principal component analysis (PCA) was adopted to develop a predictive model of the AsAA surgery.

PATIENTS AND METHODS

Study Population

The study population consisted of 125 patients with AsAA and different aortic valve morphotypes followed in our hospital institution. All patients were referred for aneurysm size evaluation by echocardiography and computed-tomography angiography (CTA). Thus, patients were categorized into 2 groups depending on valve phenotype (BAV AsAA, n=42 and TAV AsAA, n=83). Blood samples were also collected prior to CTA imaging for biomarker analysis. To reduce the impact of confounding variables influencing the development of an AsAA, we included patients with normal left ventricular ejection fraction (> 55%), and no left ventricular dilatation. Patients with both severe aortic stenosis and regurgitation were excluded. Patients with evidence of uncontrolled stage II hypertension were also excluded, although patients with history of hypertension but well controlled values on medical therapy were enrolled. The primary end point was surgical repair of aorta and/or valve for elective referral (ie, 5.5 cm for TAV AsAA and 5 cm for BAV AsAA, approximately). The decision of surgical repair was also influenced by common risk factors such as patient age, comorbidities, family history as well as the presence of significant aortic valvular diseases developed during the period of investigation. Surgically-repaired patients shared the homogeneity of surgical timing and preference as procedures were

done by the same surgeon (M.P.). The study was approved by our institutional review board (IRRB/04/14), and all patients gave informed consent prior to study enrolment.

MicroRNA Profiling and Protein Biomarkers

Circulating expression levels (versus healthy aorta of 18 volunteers) of exosomal miRNAs and absolute levels of matrix metalloproteinases (MMP-1, -2, -3, -7, -8, -9, -12 and -13) and tissue inhibitors (TIMP-1, -2, -3 and -4) were evaluated as described previously by our group [7]. miRNAs were selected because of their association with aortopathy [15] and involvement with the regulation of specific protein targets within the cardiovascular system like several MMPs and ECM components here investigated.

In brief, 10 ml of blood was collected in a serum separator tube prior to CTA imaging and then the serum was obtained for exosome isolation. RNA was extracted from the exosomal pellet while the purity of isolated RNA was determined by OD260/280 using a Nanodrop ND-1000 (Thermo Scientific, Worcester, MA). Thus, microRNA profiling was done using Custom TaqMan® Array MicroRNA Cards with 47 miRNAs (Thermo Fisher Scientific, Worcester, MA) for sample and performed with Applied Biosystems 7900 HT Real-Time PCR system. Each real-time PCR session was 3-4 hours long at rough cost of €300 per patient. Expression data of miRNA was normalized to U6 snRNA, using the 2-ΔΔCT method, with the pool of normal samples from 18 healthy individual as reference samples.

Serum concentration of human activated TGF-β and s-RAGE proteins were quantified by enzyme-linked immunosorbent assay (ELISA), with results calculated by reference to the standard curves. Luminex technology was adopted to measure the serum concentration of MMPs and TIMPs, following the manufacturer's instructions (Thermo Fisher Scientificc, Worcester, MA).

In-Vivo Strain Analysis

Strain analysis of AsAA wall mechanics at peak systole by CTA was done using an algorithm previously developed by our group [16] in the mathematical language software MATLAB (v2018, Mathworks, MA, USA). As compared to our previous studies on intramural stress of AsAAs [10, 17, 18], we preferred to quantify the aortic strain of the aneurysmal wall since this descriptor is independent of the choice of material properties with respect to stress.

To quantify aortic wall strain, CTA images were used to reconstruct the aortic wall at both end-diastolic and peak-systolic cardiac phases using the medical imaging software Mimics (Mimics v20, Materialise, Leuven, BE). The surface describing the diastolic aortic-luminal surface was then projected normally onto the systolic aortic-luminal surface to determine the displacement field as the Euclidean distance between closest points. Thus, the relative displacement of the aortic wall characterizes the diastolic-to-systolic displacement field if the diastole is assumed as the baseline configuration. For each point of the aneurysmal wall, the systolic strain distribution can be therefore computed as the ratio of the relative displacement to the baseline configuration (ie, the aortic luminal surface at diastole).

In-Silico Flow Analysis

Computational flow analyses were carried out using an approach previously developed by our group [10] to study the hemodynamics of AsAAs by considering the aortic valve shape at systole. The virtual models of each AsAA were reconstructed using semi-automatic segmentation of CTA images with the largest aortic valve opening area. To evaluate shear stress, AsAA reconstructions representing the fluid domain were meshed with unstructured tetrahedral elements at spatial resolution of 0.3x0.3x0.3 mm. The blood was assumed as an incompressible laminar-flow fluid with non-Newtonian viscosity described by the Carreau model.

To include patient-specific hemodynamics, the transaortic jet velocity evaluated by Doppler echocardiography was set as the inflow velocity condition at aortic valve. For each outlet, we first computed the global vascular resistance and arterial compliance of each patient from echocardiographic measurements and clinical demographic data. Then, these parameters were used to compute the outflow boundary conditions of a three-element Windkessel model coupled to each outflow branch. Boundary conditions were adjusted to match brachial artery pulse pressure. The Navier–Stokes equations governing fluid motion were solved with an implicit algorithm in FLUENT v19 (ANSYS Inc., Canonsburg, PA, USA), which has been previously used to resolve high-frequency, time-dependent flow instabilities encountered in complex cardiovascular anatomies [19, 20].

Morphological, Structural and Hemodynamic Variables

For all patients, aortic diameters were measured at the sinus of Valsalva (D_{sinus}), sinotubular junction (D_{STJ}), and mid-ascending aorta (D_{asc}). As a measure of the physiological aortic compliance, the pressure-strain modulus was also calculated as: PSmod = Ddias(Psys - Pdias)/(Dsys - Ddias) where Dsys and Ddias are the systolic and diastolic aortic diameters, and Psys and Pdias the systolic and diastolic blood pressures measured by brachial sphygmomanometer (see Table 1). Aortic wall strain, peak systolic WSS and time-averaged WSS (TAWSS) over one cardiac cycle were obtained for the entire thoracic aorta, with further in-depth subanalysis in the ascending aorta by computing the mean value around circumferences placed at sinus of Valsalva, sinotubular junction as well as at the proximal, mid and distal ascending aorta.

A total of 76 variables including 47 circulating miRNAs, 14 protein biomarkers, 8 hemodynamic variables, 4 aortic wall strain measurements and 7 anatomical measurements were investigated for each patient.

Statistical Analysis

Data are shown as mean±standard deviation or percentage (number) depending on the variable distribution. Mann-Whitney test was used to compare variables between BAV AsAA and TAV AsAA while the X^2 test was adopted to analyze frequencies. Pearson's correlation was performed to identify linear relationships of circulating miRNA expression, MMP and TIMPs, with biomechanical parameters (ie, WSS and aortic wall strain) and physiological parameters as the PSmod. Bonferroni's correction was performed for multiple testing.

In addition, PCA was performed for dimensionality reduction of all data computed for each patient. Before PCA, the data were scaled to unit variance and mean centered. First 3 principal components (PC1 to 3) were analyzed to assess separation between monitored versus surgically-operated patients. The tolerance ellipse based on Hotelling's T2 at a significance level of 0.05 was calculated and shown in the score plots. After data reduction, the most important variables were retained and used in a logistic regression model to identify which parameters were predictive of aortic surgery. The receiver operating characteristic (ROC) curves were plotted and the area under the ROC curve was calculated as an index of the predictive value of the regression model. Statistical analyses were performed using SPSS software (IBM SPSS Statistics v.17, New York, NY), with all probability values considered significant at 0.05 threshold.

RESULTS

Table 1 summarizes patient demographics. The distribution of aortic diameter measurements in BAV AsAAs did not significantly differ from that of TAV AsAAs at level of sinus (p=0.781), sino-tubular junction (p=0.884) and mid-ascending aorta (p=0.169). There was a significant difference in the age of BAV AsAAs versus TAV AsAAs (p=0.002), with male predominance of

88% in bicuspid patients. During the enrollment period, elective surgical repair of dilated aorta was carried out for 8 BAV AsAAs and 13 TAV AsAAs patients with aortic diameters of 49.4±4.3 mm and 52.1±3.9 mm, respectively. Elective surgical repair was mostly influenced by concomitant indications for cardiac surgery due to the presence of aortic valvular stenosis or insufficiency developed during the period of enrollment. Out of n=21 surgically-operated AsAAs, n=15 patients had both AsAA and aortic valve replacements while only n=6 patients received an isolated ascending aortic replacement due to the presence of relevant aortic growth rate (n=4) or other aortic risk factors (n=2). Emergent aortic surgery or death due to aortic rupture/dissection were not present.

Local maximal *in-vivo* aortic wall strain was found in the major curvature of the aneurysmal aorta without showing difference between bicuspid and tricuspid patients (Figure 1A and B). Maps of peak systolic WSS revealed high magnitudes in regions just above the sino-tubular junction (namely, analysis plane = AA1) and mid-ascending aorta (AA2) as compared to those of sinus and distal ascending aorta (AA3) (Figure 2A and B). Specifically, mean values of systolic WSS and TAWSS on each analysis plane were significantly increased from the sino-tubular junction to the mid-ascending aorta of BAV AsAAs when compared with those of TAV AsAAs (Figure 3A). There was no significant difference in the mean values of the aortic wall strain in all analysis planes between BAV AsAAs and TAV AsAAs.

A significant difference was observed in the expression levels of miR-133a ($p = 0.038$), miR-320a ($p = 0.014$) and miR-34a ($p = 0.010$) of BAV AsAA versus TAV AsAA, and this suggests that the circulating exosomal expression of these miRNAs different depending on valve morphotype (Figure 3B). Among MMPs, the absolute levels of MMP-2 and MMP-13 of BAV AsAAs were the only protein showing a significant difference with that of TAV AsAAs (2806±201

ng/ml for BAV AsAA versus 2509±136 for TAV AsAA, p=0.031 for MMP-2 and 1169±119 ng/ml for BAV AsAA versus 2217±256 for TAV AsAA, p=0.013 for MMP-13).

Pearson's correlation revealed several relationships between shear stress and protein activity for AsAAs, irrespective of valve phenotype. At analysis plane of proximal aorta, the plasma levels of MMP-1 and TIMP-1 were positively correlated to peak systolic WSS and TAWSS whereas the MMP-2 was positively related to TAWSS (Figure 4). At sinus of Valsalva, MMP-1 and TIMP-1 were positively correlated to both peak systolic WSS and TAWSS (eg, R=0.32, p=0.005, for WSS and R=0.31, p=0.006 for TAWSS for MMP-1). At mid-ascending aorta (AA2), the protein level of TIMP-4 was positively correlated to peak systolic WSS (R=0.31, p=0.017). There was no correlation between aortic wall strain and biomarkers. The aortic diameter of patients with AsAA was correlated with MMP-1 (R=0.24, p=0.031), MMP-2 (R=0.45, p=0.020) and strain at mid-ascending aorta (R=-0.22, p=0.041).

When analyses were restricted to the BAV AsAAs, the aortic wall strain at mid-ascending aorta was positively correlated to the plasma level of miR-320a (Figure 5A) and miR-26a (R=0.55, p=0.041) while the bicuspid-induced WSS was correlated to the MMP-7 (Figure 5C). The only statistically-significant inverse correlation was observed between the peak systolic WSS and the exasomal level of miR-29a (Figure 5B). A significant relationship was found between the stiffness at the mid-ascending aorta as measured by PSmod and the absolute level of MMP-7 (Figure 5C). There was not any correlation between the aortic diameter and investigated variables for bicuspid patients.

A PCA based on the expression of the identified biomarkers, shear stress, aortic wall strain and demographics data showed no separation of patients who underwent surgery from those

currently monitored, when analyzing BAV and TAV patients together (Figure 6). However, the loading plot revealed that the most important variables responsible for AsAA surgery were age, MAP, diastolic pressure (Pdias), WSS, MMP-1, TIMP-1 and MMP-12. Following this, a logistic regression model including shear stress and biomarkers was developed to determine the probability of aortic surgery in our patient population, and then the ROC curve was calculated (see Figure 7). The combination of systolic WSS, MMP-1, TIMP-1 and MMP-12 resulted in the predictive value of AUC=0.898.

COMMENT

In this study, we documented direct correlations of both shear stress and aortic wall strain to circulating levels of exasomal miRNA analytes and protein activity in the aneurysmal ascending aorta of patients with BAV and TAV. In a large data set of 125 patients, we observed that a) wall shear stress and strain are pronounced in the proximal ascending aorta from the sino-tubular junction to the mid-ascending aorta; b) aortic valve morphology differently modulates exosomal miRNA analytes (ie, miR-133a, miR-320 and miR-34a); c) as the shear stress increases in the proximal aneurysmal aorta, the plasma protein activity of MMP-1, TIMP-1 and MMP-2 increases; d) for BAV AsAAs, the strain at mid-ascending aortic wall is associated to an up-regulation of plasma levels of both miR-320 and miR-26a while the WSS to a down-regulation of miR-29a; e) a combination of non-invasive shear stress and circulating biomarkers can potentially predict the event of AsAA surgery with a high degree of specificity and sensitivity.

Studies on the association between abnormal shear stress and aortic wall remodeling as a contributing factor in the development of AsAA are lacking and mainly focused on 4D Flow MRI and post-surgery histology [13, 14]. In a different way, the role of imaging and biomarkers in AsAAs was separately investigated by several research groups. Measurements of plasma levels of MMPs and TIMPs in AsAAs evinced differences between BAV AsAA and TAV AsAA [5]

whereas the protein activity of MMP-2 was found as a biomarker of the aortic dilatation in BAV patients [6]. *In-vivo* imaging studies based on 4D Flow MRI have widely demonstrated that the flow jet dictated by the bicuspid morphology locally impinges the aneurysmal aortic wall in BAV AsAAs, portending to regional WSS-related stimulus on the diseased vessel [9, 12]. To our knowledge, this is the first study documenting therelationship of the shear stress with circulating plasma levels of MMP-1, TIMP-1 and MMP-2 (see Figure 4) in a large cohort of patients with AsAAs and not any remarkable valve dysfunction. This supports direct evidence for which local alterations of shear stress exerted on the AsAA wall can lead to change in the aortic structure, ultimately portending adverse vascular remodeling by mechanotransduction.

During the past years, miRNAs have emerged as promising biomarker of vascular and heart remodeling [15] , as these molecules mediate the expression of key components of signal transduction at multiple levels. Initial findings have demonstrated that vascular remodeling of AsAAs was associated to the altered blood plasma level of miR-17 in severely- versus less-dilated ascending aortas [21] and to altered levels of miR-29a in BAV AsAA versus TAV AsAA [22]. Most importantly, miRNAs are responsive to fluid shear by potentially trigging tissue maladaptation, and this can explain the relationship between the down-regulation of miR-29a and the decrease of WSS found in this study for BAV AsAAs. The proposed biomechanical properties (ie, WSS and strain) highlighted several relationships with miRNAs and other biomarkers. This is likely caused by the fact thatthese molecules can bind protein proteolytic activity in AsAA as we reported interaction of miR133a and miR-320 with MMP-3 and MMP-9 [7]. The majority of the miRNAs here reported can target aortic pathways that are involved in proliferation and apoptosis (miR-320 and miR133a), vascular smooth muscle cells (miR-26a), and ECM structure/function (miR133a and miR-34a). There is however a limited literature on the potential link between miRNAs and biomechanical descriptors. For instance, Akerman et al. [23] demonstrated that elevated intramural stress can result in the reduction of miR133a in

descending thoracic aortas (mouse models). Although a huge work is needed to identify potential miRNA signature for risk stratification of aortopathy, we speculated that shear-dependent miRNAs and their potential to impair vascular mechanics (as reflected by strain) have the potential to fill the gap between genetic and hemodynamic factors determining the pathogenesis of aneurysm development and progression.

A combination of imaging-derived metrics of flow-related WSSs and circulating biomolecule-based risk markers have the potential of taking aneurysm risk definition to a highly individualized level. Using logistic regression after PCA-based data dimensionality reduction, the feasibility of such a precision medicine approach was demonstrated by the capability of our model (AUC=0.898) to predict the event of AsAA surgery using a combination of WSS measurements and circulating biomarkers (ie, MMP-1, TIMP-1, MMP-12) (see Figure 7). It should be noted that aortic diameter at the time of surgery was 49.4±4.3 mm for BAV AsAAs (n.8 patients) and 52.1 ±3.9 mm for TAV AsAAs (n.13 patients) with the presence of aortic valve dysfunction in all cases except for six patients. Therefore, the limited number of surgically-repaired patients and the clinical variables confounding the decision for surgery may have masked important findings. We also did not account for differences in biomarkers, hemodynamic and structural variables that can likely occur when aneurysms are grouped according to the pattern of aortic dilatation. This can influence the predictive capability of the proposed model. To develop a personalized approach for individual or subgroups of patients with AsAAs, several predictive models should be developed stratifying patients according to the aortic phenotype (ie, aortic root dilatation versus ascending phenotype) or aortic valve morphology (BAV versus TAV) whereas machine learning algorithms could be adopted to better interpret the large amount of biomarker and biomechanical data here proposed.

Although study limitations such as verification of *in-silico* WSSs by 4D Flow MRI, validation of miRNA analytes on aortic tissues, selection bias and a restricted number of surgically-repaired patients with AsAAs, we reported direct relationships of both shear stress and strain exerted on the aneurysmal aortic wall with circulating exasomal miRNAs and protein proteolytic activity. We also demonstrated the feasibility to combine imaging-derived metrics and circulating biomarkers to predict the risk of aortic surgery towards on a holistic and personalized decision-making process of the aortic wall disease. Future studieswith large patient numbers and long follow-up are needed to fully explore the association of biomechanical descriptors and circulating biomarkers with the aortic growth and clinical outcome of patients with AsAAs.

REFERNCES

1. Coady MA, Rizzo JA, Goldstein LJ, Elefteriades JA. Natural history, pathogenesis, and etiology of thoracic aortic aneurysms and dissections. Cardiol Clin 1999;17(4):615-635; vii.
2. Masri A, Kalahasti V, Alkharabsheh S et al. Characteristics and long-term outcomes of contemporary patients with bicuspid aortic valves. J Thorac Cardiovasc Surg 2016;151(6):1650-1659 e1651.
3. Michelena HI, Khanna AD, Mahoney D et al. Incidence of aortic complications in patients with bicuspid aortic valves. JAMA 2011;306(10):1104-1112.
4. Rueda-Martinez C, Lamas O, Carrasco-Chinchilla F et al. Increased blood levels of transforming growth factor beta in patients with aortic dilatation. Interact Cardiovasc Thorac Surg 2017;25(4):571-574.
5. Ikonomidis JS, Ivey CR, Wheeler JB et al. Plasma biomarkers for distinguishing etiologic subtypes of thoracic aortic aneurysm disease. Journal of Thoracic and Cardiovascular Surgery 2013;145(5):1326-1333.
6. Wang Y, Wu B, Dong L, Wang C, Wang X, Shu X. Circulating matrix metalloproteinase patterns in association with aortic dilatation in bicuspid aortic valve patients with isolated severe aortic stenosis. Heart Vessels 2016;31(2):189-197.
7. Gallo A, Agnese V, Coronello C et al. On the prospect of serum exosomal mirna profiling and protein biomarkers for the diagnosis of ascending aortic dilatation in patients with bicuspid and tricuspid aortic valve. International Journal of Cardiology 2018;https://doi.org/10.1016/j.ijcard.2018.10.005.
8. Balistreri CR, Crapanzano F, Schirone L et al. Deregulation of notch1 pathway and circulating endothelial progenitor cell (epc) number in patients with bicuspid aortic valve with and without ascending aorta aneurysm. Scientific reports 2018;8(1):13834.

9. Mahadevia R, Barker AJ, Schnell S et al. Bicuspid aortic cusp fusion morphology alters aortic three-dimensional outflow patterns, wall shear stress, and expression of aortopathy. Circulation 2014;129(6):673-682.
10. Pasta S, Gentile G, Raffa GM et al. In silico shear and intramural stresses are linked to aortic valve morphology in dilated ascending aorta. European Journal of Vascular and Endovascular Surgery 2017;S1078-5884(17)30331-3.
11. Youssefi P, Gomez A, He T et al. Patient-specific computational fluid dynamics-assessment of aortic hemodynamics in a spectrum of aortic valve pathologies. J Thorac Cardiovasc Surg 2017;153(1):8-20 e23.
12. van Ooij P, Markl M, Collins JD et al. Aortic valve stenosis alters expression of regional aortic wall shear stress: New insights from a 4-dimensional flow magnetic resonance imaging study of 571 subjects. Journal of the American Heart Association 2017;6(9).
13. Guzzardi DG, Barker AJ, van Ooij P et al. Valve-related hemodynamics mediate human bicuspid aortopathy: Insights from wall shear stress mapping. J Am Coll Cardiol 2015;66(8):892-900.
14. Bollache E, Guzzardi DG, Sattari S et al. Aortic valve-mediated wall shear stress is heterogeneous and predicts regional aortic elastic fiber thinning in bicuspid aortic valve-associated aortopathy. Journal of Thoracic and Cardiovascular Surgery 2018;156(6):2112-+.
15. Pulignani S, Borghini A, Andreassi MG. Micrornas in bicuspid aortic valve associated aortopathy: Recent advances and future perspectives. J Cardiol 2019;74(4):297-303.
16. Pasta S, Agnese V, Di Giuseppe M et al. In-vivostrain analysis of dilated ascending thoracic aorta by ecg-gated ct angiographic imaging. Annals of Biomedical Engineering 2017;45(12):2911-2920.
17. Rinaudo A, D'Ancona G, Lee JJ et al. Predictingoutcome of aortic dissection with patent false lumen by computational flow analysis. Cardiovasc Eng Technol 2014;5(2):176-188.

18. Rinaudo A, Pasta S. Regional variation of wallshear stress in ascending thoracic aortic aneurysms. Proceedings of the Institution of Mechanical Engineers Part H, Journal of engineering in medicine 2014;228(6):627-638.
19. D'Ancona G, Amaducci A, Rinaudo A et al. Haemodynamic predictors of a penetrating atherosclerotic ulcer rupture using fluid–structure interaction analysis. Interactive CardioVascular and Thoracic Surgery 2013;17(3):576-578.
20. Lee JJ, D'Ancona G, Amaducci A, Follis F, Pilato M, Pasta S. Role of computational modeling in thoracic aortic pathologies -a review. Journal of Cardiac Surgery 2014;29(5):653-662.
21. Girdauskas E, Petersen J, Neumann N et al. Evaluation of microribonucleic acids as potential biomarkers in the bicuspid aortic valve-associated aortopathydagger. Interact Cardiovasc Thorac Surg 2018.
22. Jones JA, Stroud RE, O'Quinn EC et al. Selective microrna suppression in human thoracic aneurysms: Relationship of mir-29a to aortic size and proteolytic induction. Circulation Cardiovascular genetics 2011;4(6):605-613.
23. Akerman AW, Blanding WM, Stroud RE et al. Elevated wall tension leads to reduced mir-133a in the thoracic aorta by exosome release. Journal of the American Heart Association 2019;8(1):e010332.

Figure Legends

Figure 1: Distribution of aortic wall strain in (A) BAV AsAA and (B) TAV AsAA.

Figure 2: Distribution of systolic WSS in (A) BAV AsAA and (B) TAV AsAA.

Figure 3: Comparison of (A) TAWSS and (B) miRNAs between BAV AsAA and TAV AsAA; shear stress computed at sinus, STJ, AA1, AA2 and AA3; * significantly different from TAV AsAA ($P<0.05$).

Figure 4: (A) Correlation between WSS and MMP-1, (B) TAWSS and TIMP-1 and (C) TAWSS and MMP-2; WSS measured at AA1.

Figure 5: (A) Correlation of strain with miR-320a; WSS with (B) miR-29a and (C) MMP-7; (D) PSmod with MMP-7; values obtained at AA1 for BAV AsAA.

Figure 6: Two-dimensional score plots of (A) PC1 versus (A) PC2 versus PC3 with loading showing key variables responsible for clustering surgically-repaired patients (red dots) vs monitored-patients (black dots); the PC1 to PC2 plot shows age, MAP, diastolic pressure (Pdias), MMP-12 as variables; the PC1 to PC2 plot shows WSS, MMP-1 and TIMP-1 as variables; solid lines represents 95% tolerance ellipse.

Figure 7: ROC curve for the model combining WSS, MMP-1, TIMP-1 and MMP-12 to predict the probability of aortic surgery.

Table 1: Descriptive statistics of patient demographics

	BAV AsAA (n=42)	TAV AsAA (n=83)	p-value
Age (years)	57.8±11.4	64.6±10.5	0.002
Male *(%)*	88.1	73.5	
Surgery *(%)*	23.8	35.9	
BSA (m^2)	3.4±6.0	2.6±3.8	0.300
Psys (mmHg)	136.7±12.9	135.6±14.1	0.598
Pdias (mmHg)	76.7±10.6	75.2±8.5	0.353
MAP (mmHg)	93.1±10.1	92.1±8.2	0.475
SV (ml)	76.8±29.7	75.1±25.9	0.921
CO (ml/min)	5440.5±2157.9	5503.6±2184.6	0.715
Hyper *(%)*	66.7	68.8	
AI *(%)*			
None	3.2	17.8	
Mild	12.9	63.3	
Moderate	64.8	10.0	
Severe	19.0	8.9	
AS *(%)*			
None	37.5	/	
Mild	47.5	/	
Moderate	15.0	/	
Aortic FlowJet *(m/s)*	1.9±0.7	1.4±0.4	0.001
Orifice Area *(mm^2)*	344.9±87.6	336.0±97.3	0.285
Aortic Diameters *(mm)*			
Sinus	41.5±5.8	42.2±5.7	0.781
STJ	36.1±5.1	36.5±4.7	0.884
Mid-Ascending Aorta	44.4±5.9	43.9±4.8	0.169
PSmod *(kPa)*			
Sinus	475.8±570.9	541.1±915.3	0.349
STJ	270.1±269.8	566.6±1265.2	0.074
Mid-Ascending Aorta	1346.4±3567.6	983.2±2870.2	0.907

Note: BSA=body surface area; Psys=systolic blood pressure; Pdias=diastolic blood pressure; MAP=mean arterial pressure; SV=stroke volume; CO=cardiac output; Hyper=hypertension; AI=aortic insufficiency; AS=aortic stenosis; STJ=sino-tubular junction; PSmod=pressure-strain modulus;

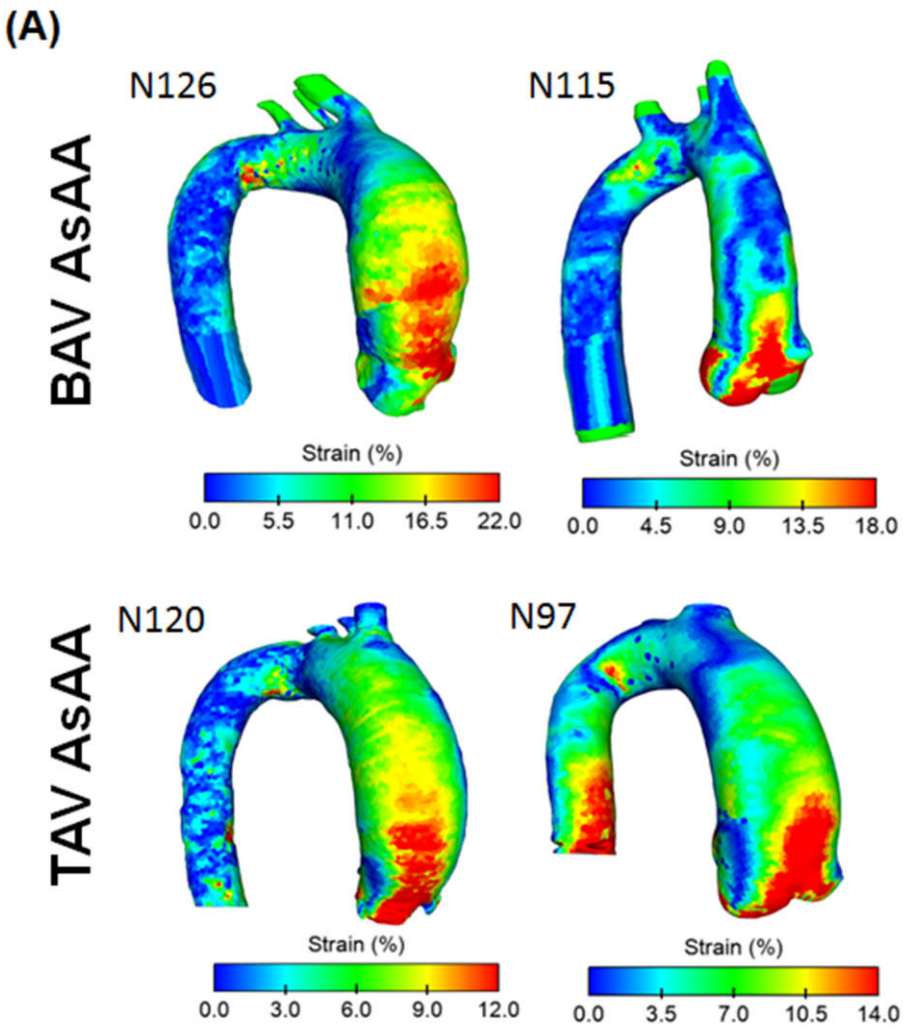
(A)
BAV AsAA
N126
N115
Strain (%)
0.0 5.5 11.0 16.5 22.0
Strain (%)
0.0 4.5 9.0 13.5 18.0
TAV AsAA
N120
N97
Strain (%)
0.0 3.0 6.0 9.0 12.0
Strain (%)
0.0 3.5 7.0 10.5 14.0

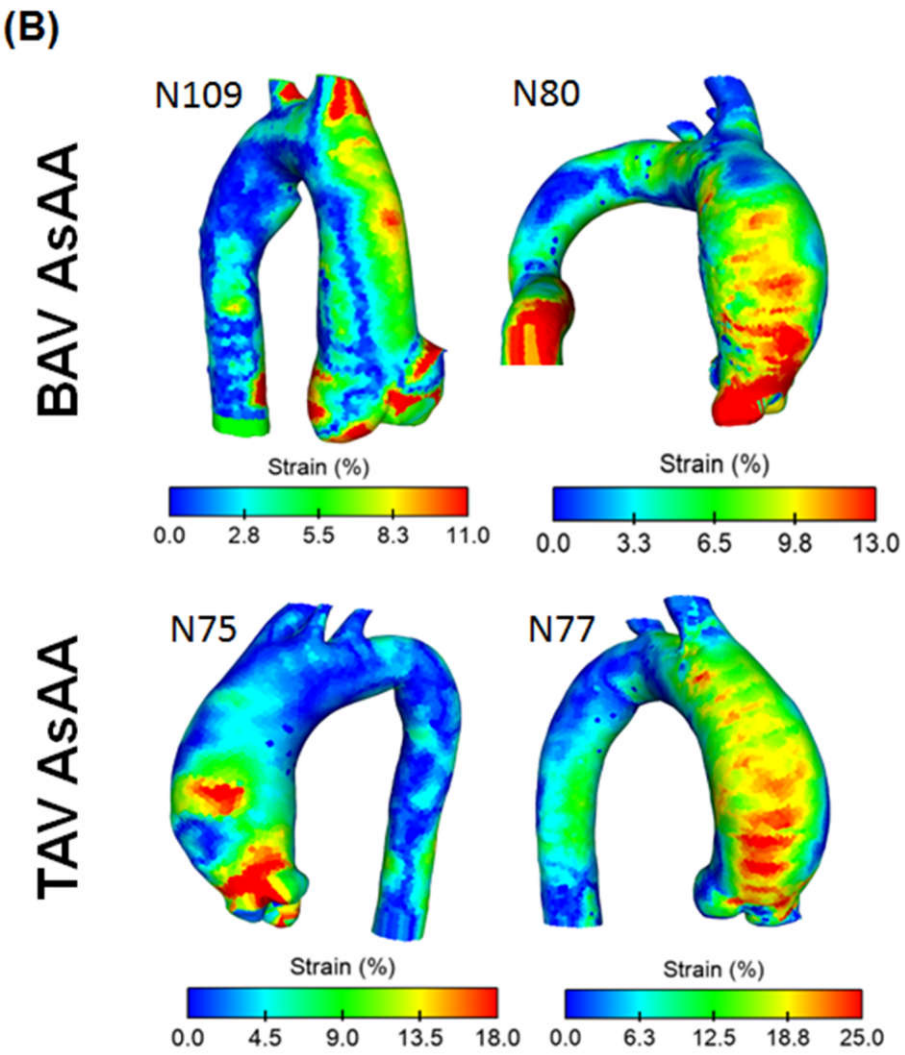
(B)
BAV AsAA
N109
N80
Strain (%)
0.0 2.8 5.5 8.3 11.0
Strain (%)
0.0 3.3 6.5 9.8 13.0
TAV AsAA
N75
N77
Strain (%)
0.0 4.5 9.0 13.5 18.0
Strain (%)
0.0 6.3 12.5 18.8 25.0

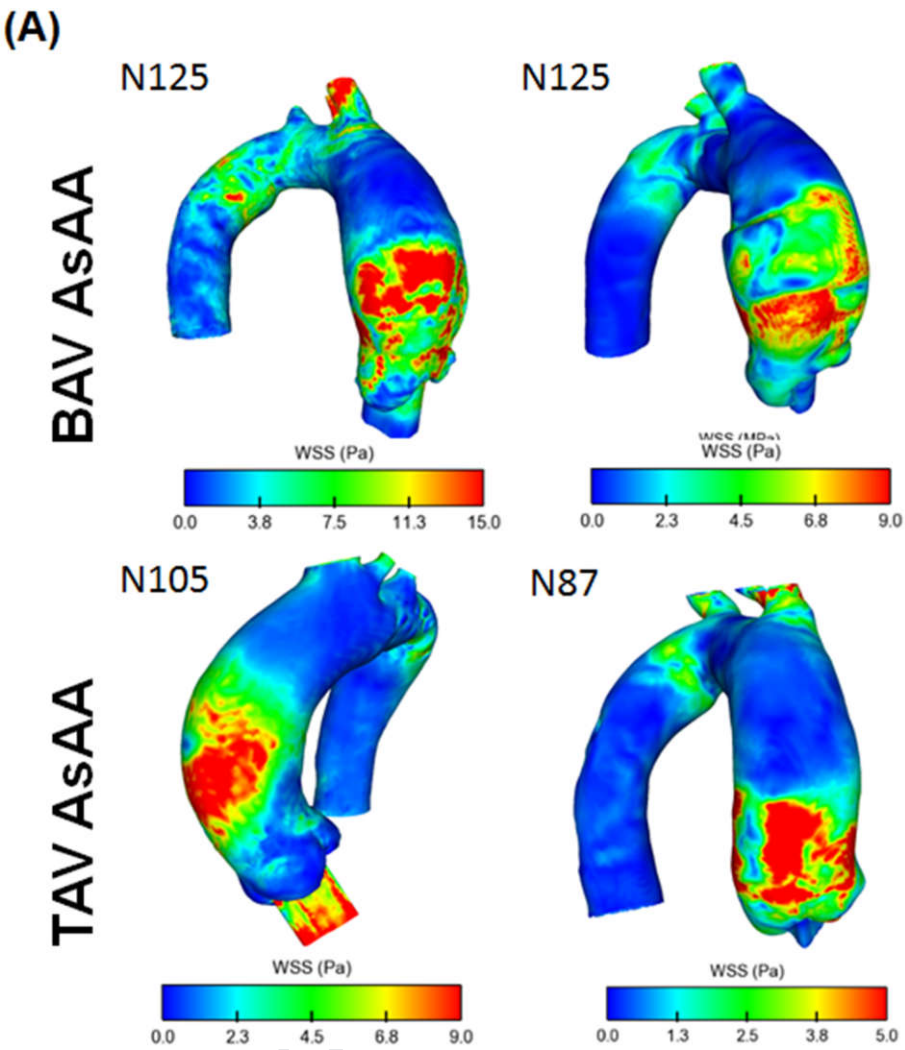
(A)
N125
N125
BAV AsAA
WSS (Pa)
0.0 3.8 7.5 11.3 15.0
WSS (Pa)
0.0 2.3 4.5 6.8 9.0
N105
N87
TAV AsAA
WSS (Pa)
0.0 2.3 4.5 6.8 9.0
WSS (Pa)
0.0 1.3 2.5 3.8 5.0

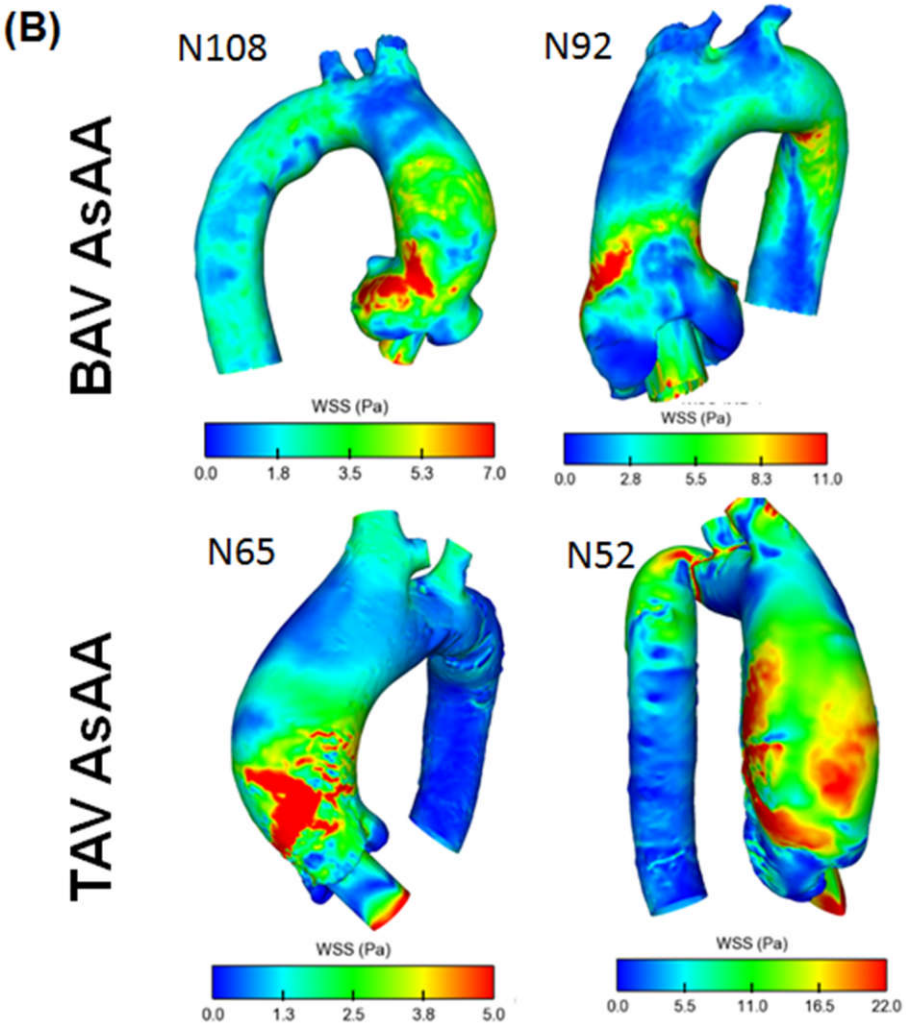
(B)
BAV AsAA
TAV AsAA
N108
N92
N65
N52
WSS (Pa)
0.0 1.8 3.5 5.3 7.0
WSS (Pa)
0.0 2.8 5.5 8.3 11.0
WSS (Pa)
0.0 1.3 2.5 3.8 5.0
WSS (Pa)
0.0 5.5 11.0 16.5 22.0

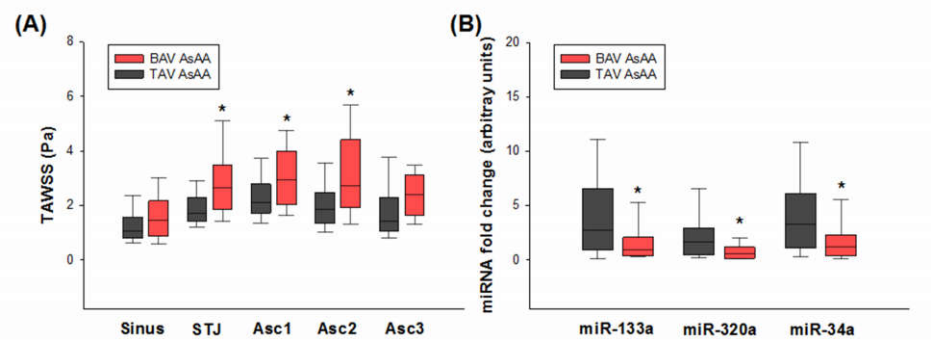

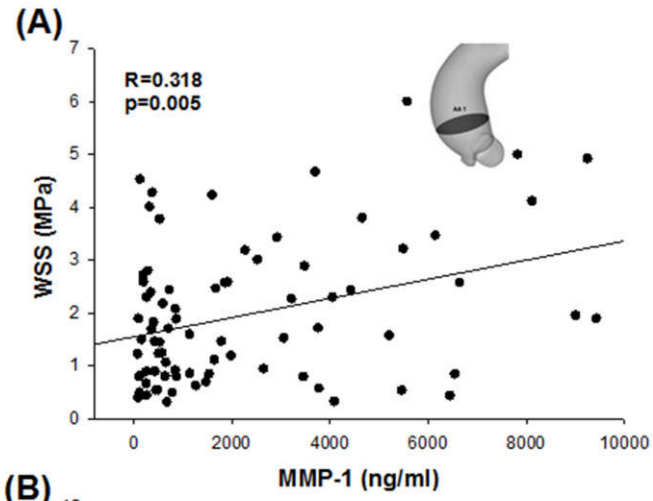
(A)
R=0.318
p=0.005
WSS (MPa)
MMP-1 (ng/ml)
0
1
2
3
4
5
6
7
0
2000
4000
6000
8000
10000

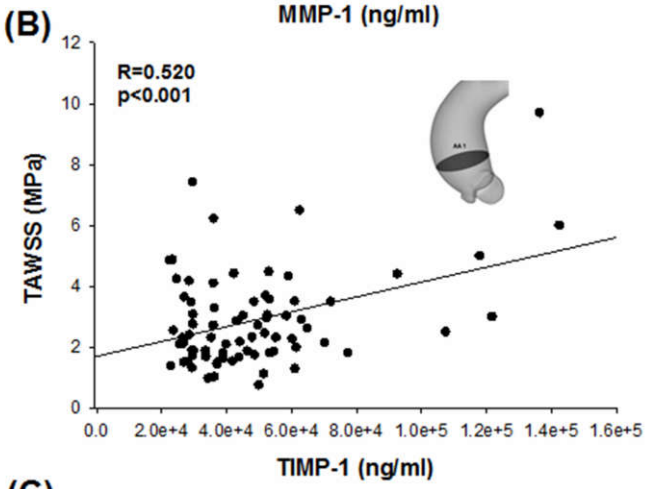
(B)
R=0.520
p<0.001
TAWSS (MPa)
TIMP-1 (ng/ml)
0
2
4
6
8
10
12
0.0
2.0e+4
4.0e+4
6.0e+4
8.0e+4
1.0e+5
1.2e+5
1.4e+5
1.6e+5

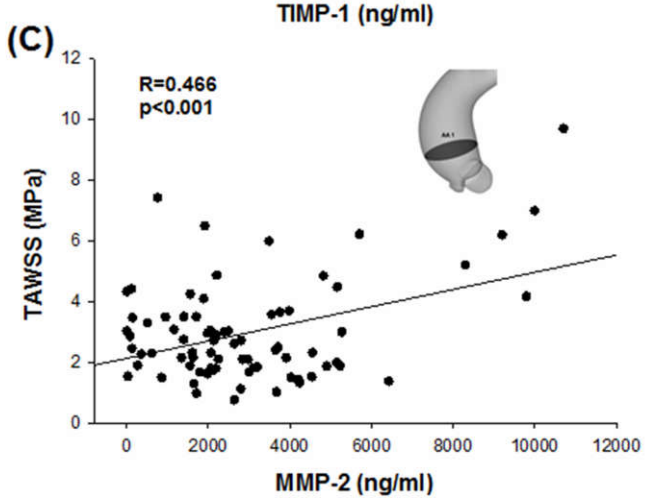
(C)
R=0.466
p<0.001
TAWSS (MPa)
MMP-2 (ng/ml)
0
2
4
6
8
10
12
0
2000
4000
6000
8000
10000
12000